https://doi.org/10.1595/205651323X16813753335431 *Johnson Matthey Technol. Rev.*, 2023, **67**, (4), 438–448

JOHNSON MATTHEY
TECHNOLOGY REVIEW

technology.matthey.com

Impact of Solution Chemistry on the Biotechnological Synthesis and Properties of Palladium Nanoparticles

Palladium solution chemistry plays an important role in the bioreduction of Pd(II)

Christopher Egan-Morriss*
Williamson Research Centre for Molecular Environmental Science, Department of Earth and Environmental Sciences, The University of Manchester, Oxford Road, Manchester, M13 9PL, UK

Richard L. Kimber
Department of Environmental Geosciences, Centre for Microbiology and Environmental Systems Science, University of Vienna, 1090, Vienna, Austria

Nigel A. Powell
Johnson Matthey, Blounts Court, Sonning Common, Reading, RG4 9NH, UK

Jonathan R. Lloyd**
Williamson Research Centre for Molecular Environmental Science, Department of Earth and Environmental Sciences, The University of Manchester, Oxford Road, Manchester, M13 9PL, UK

Email:
*christopher.eganmorriss@manchester.ac.uk;
**jon.lloyd@manchester.ac.uk

PEER REVIEWED

Received 20th January 2023; Revised 27th March 2023; Accepted 11th April 2023; Online 13th April 2023

The biosynthesis of palladium nanoparticles supported on microbial cells (bio-Pd) has attracted much recent interest, but the effect of solution chemistry on the process remains poorly understood. Biological buffers can be used to maintain physiological pH during the bioreduction of Pd(II) to Pd(0) by microbial cells, however, buffer components have the potential to complex Pd(II), and this may affect the subsequent microbe-metal interaction. In this study, a range of Pd(II) salts and biological buffers were selected to assess the impact of the solution chemistry on the rate of bioreduction of Pd(II) by *Geobacter sulfurreducens*, and the resulting biogenic palladium nanoparticles. The different buffer and Pd(II) combinations resulted in changes in the dominant Pd(II) species in solution, and this affected the amount of palladium recovered from solution by the microbial cells. The physical properties of the bio-Pd nanoparticles were altered under different solution chemistries; only slight variations were observed in the mean particle size (<6 nm), but significant variations in particle agglomeration, the extent of Pd(II) bioreduction and subsequent catalytic activity for the reduction of 4-nitrophenol (4-NP) were observed. The combination of sodium tetrachloropalladate and bicarbonate buffer resulted in bio-Pd with the smallest mean particle size, and the fastest initial rate of reaction for 4-NP reduction (0.33 min^{-1}). Other solution chemistries appeared to damage the cells and result in bio-Pd with relatively poor catalytic performance. This work emphasises

that future studies into bio-Pd synthesis should consider the importance of solution chemistry in controlling the speciation of Pd(II) and its impact on both the bioreduction process and the resulting properties of the nanoparticles produced, in order to maximise Pd(II) biorecovery and optimise catalytic properties.

1. Introduction

Metal nanoparticle synthesis by microorganisms is a relatively simple, economical, scalable and green biotechnology (1). Palladium nanoparticles supported on microbial cells (bio-Pd) are of particular interest as they have shown strong performance as heterogeneous catalysts towards industrially important reactions, including hydrogenation, hydrogenolysis and C–C couplings such as Heck and Suzuki reactions (2). Bio-Pd is synthesised *via* enzymatic reduction of Pd(II) to Pd(0) at ambient temperature, and requires only the cultured microbes, a Pd(II) source, inexpensive buffer solutions and an electron donor, such as organic acids or hydrogen (3–6). The effect of using different microbes in bio-Pd synthesis has been examined previously (7), however, few studies have tried to assess the impact of other synthesis factors on the formation and properties of bio-Pd. Arguably one of the most important and overlooked factors in bio-Pd synthesis is the effect of solution chemistry. Pd(II) speciation in aqueous solutions is a complex topic (8–10), as Pd(II) is a strongly hydrolysable metal (11). Sodium tetrachloropalladate is the most commonly used Pd(II) salt in bio-Pd synthesis, but studies often fail to take into account that microbes will not come into contact with the tetrachloropalladate ion $[PdCl_4]^{2-}$ complex (TCP), as under typical reaction conditions of low chloride concentration and near-neutral pH, it undergoes fast hydrolysis to $[PdCl_3(H_2O)]^-$. This will transform further *via* hydrolysis and deprotonation to hydroxy- and oxy-complexes (12). Tetraamminepalladium chloride monohydrate is also often used in palladium nanoparticle synthesis, and is of interest due to its positive charge, as tetraamminepalladium ion $[Pd(NH_3)_4]^{2+}$ (TAP), and greater stability in aqueous solution than TCP. In the context of bio-Pd synthesis, Pd(II) speciation is further complicated by potential reactions with buffer components and the cell surface, making it a challenging topic to broach.

The complexation of metals by buffers is a well-known occurrence, however most literature is concerned with biologically relevant metals (13). Few studies have focused on non-essential metals, with the notable exception of the bioreduction of Tc(VII), where different buffered and unbuffered solutions resulted in different solid-phase reduction products (14, 15). More widely, metal-buffer interactions have been investigated for nanoparticle synthesis. For example, the use of various buffers had a profound effect on gold nanoparticle size in a starch-glucose mediated synthesis (16), but did not cause significant change in size of platinum nanoparticles (17). In a peptide-mediated palladium nanoparticle synthesis process, choice of buffer significantly affected the agglomeration and size of nanoparticles. Tris buffer gave highly agglomerated particles with mean particle size 30.5 ± 4 nm, whereas (4-(2-hydroxyethyl)-1-piperazineethanesulfonic acid) (HEPES) buffer produced agglomerated chains of 75.3 ± 9 nm particles (18).

This study is the first to consider the effect of solution chemistry on the synthesis and resulting properties of bio-Pd, in the model metal-reducing bacterium *Geobacter sulfurreducens*, in this case by assessing the effect of different Pd(II) salts in selected buffers. TCP and TAP were chosen as Pd(II) salts due to their contrasting negative and positive charges, respectively, and the buffers selected were bicarbonate buffer, phosphate buffered saline (PBS) and tris buffered saline (TBS). Bicarbonate is the natural buffering component of groundwater and in human blood and has a buffer range of pH 5.4–7.4 (19). It has the advantage of being a weak complexant of Pd(II), however it is highly sensitive to CO_2 concentrations making it a relatively poor buffering agent. PBS, typical buffer range pH 7.0–7.4, is one of the most commonly used buffers in cell culture and is isotonic to mammalian and many microbial cells (20). However, the use of PBS can result in the precipitation of divalent cationic metals as insoluble phosphates. Tris buffers are common in biological laboratories as they have an effective buffer range at physiological pH 7.1–9.1. Tris is known to complex metals due to interactions with its amine group and three hydroxyl groups (Equations (i)–(iii)) (21). The combination of buffers and Pd(II) salts was selected to probe the impact of a wide range of solution chemistries on Pd(II) bioreduction by the model metal-reducing bacterium *G. sulfurreducens,* including an assessment of the effect on bio-Pd properties.

$$CO_{2(g)} + H_2O_{(l)} \rightleftharpoons H_2CO_{3(aq)} \rightleftharpoons HCO_3^-{}_{(aq)} + H^+{}_{(aq)} \quad \text{(i)}$$

$$H_2PO_4^-{}_{(aq)} \rightleftharpoons HPO_4^{2-}{}_{(aq)} + H^+{}_{(aq)} \quad \text{(ii)}$$

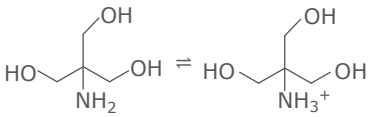

(iii)

2. Methods

2.1 Bio-Pd Synthesis

G. sulfurreducens was grown anaerobically in a defined medium (NBAF) containing acetate and fumarate as the electron donor and acceptor, respectively, at pH 7.1. Starter cultures were inoculated with a 10% by volume aliquot of late-log phase cells. The experimental culture was grown for 24 h at 30°C until late-log phase and harvested *via* centrifugation under anoxic conditions, at 4538 *g* for 20 min at 4°C. The cells were washed three times with anoxic bicarbonate buffer (30 mM) flushed with an 80:20 N_2/CO_2 mix, and were finally resuspended in the same buffer at pH 7.1.

All buffer solutions were prepared and adjusted to pH 7.2 with 4 M hydrochloric acid (HCl), added to 50 ml serum bottles and degassed and autoclaved; bicarbonate buffer (30 mM $NaHCO_3$) was purged using 80:20 gas mix of N_2:CO_2, whereas TBS (10 mM Tris base, 150 mM NaCl) and PBS (10 mM Na_2HPO_4, 1.8 mM KH_2PO_4, 137 mM NaCl, 2.7 mM KCl) were purged with N_2. Stock solutions (10 mM) of Na_2PdCl_4 and of $Pd(NH_3)_4Cl_2{\cdot}H_2O$ were made in deionised water and purged with N_2. Experimental reaction bottles were prepared by adding 1 ml of Pd(II) stock to serum bottles containing 40 ml anaerobic buffer, with acetate (10 mM) as electron donor, to give an initial Pd(II) concentration of 0.25 mM. The optical density of the washed cells was measured at 600 nm (OD_{600}) in a ultraviolet-visible (UV-vis) spectrometer, then added to reaction bottles to give a final OD_{600} of 0.5. Reaction bottles were incubated in the dark at 30°C for 24 h, and were sampled under anoxic conditions at regular time points. Bio-Pd samples were centrifuged and the supernatant assessed for palladium concentration using inductively coupled plasma mass spectrometry (ICP-MS). Post-reaction samples were washed three times *via* centrifugation with deionised water to remove the buffer salts and palladium not associated with cells. The resulting cell pellet was used for further characterisation.

2.2 Characterisation Protocols

ICP-MS was used to determine concentrations of palladium, and samples were analysed using an Agilent 7500cx ICP-MS (Agilent Technologies Inc, USA). UV-vis spectra for Pd(II) complexes in water (0.25 mM) and buffer solutions were recorded at 190–1000 nm in a UV5 UV-vis spectrometer (Mettler-Toledo, Switzerland).

Transmission electron microscopy (TEM) samples were prepared *via* drop casting of cell suspensions (2 µl) onto copper grids coated with a holey carbon film. Bright field TEM imaging was performed in a Talos F200A field emission gun (FEG) TEM (FEI Company, USA) operated at 200 kV, or in a Tecnai F30 FEG TEM (FEI Company) operated at 300 kV. Size analysis was performed on ImageJ software, 150 particles were measured per sample, with the mean of two perpendicular line measurements taken per particle.

X-ray diffraction (XRD) analysis was carried out on a D2 phaser diffractometer (Bruker, USA) with a copper Kα x-ray source (wavelength 1.54 Å). Scans were taken between 2θ values 30° and 70°. XRD analysis used the {111}, {200} and {220} peaks to identify the mean crystallite size using the Scherrer equation, FWHM = Kλ / Dcosθ, where FWHM is the full width at half-maximum of the diffraction peak, k is the shape constant, D is the crystallite size and θ is the Bragg angle.

X-ray photoelectron spectroscopy (XPS) was performed using an Axis Ultra Hybrid spectrometer (Kratos Analytical Ltd, UK) using monochromated Al Kα radiation (1486.6 eV, 10 mA emission at 150 W, spot size 300 µm x 700 µm) with a base vacuum pressure of ~5 × 10^{-9} mbar. Charge neutralisation was achieved using a filament. Binding energy scale calibration was performed using the C 1s C–C photoelectron peak at 284.8 eV. Analysis and curve fitting was performed using Voigt-approximation peaks, fitted with a Shirley background using CasaXPS processing software.

2.3 4-Nitrophenol Reduction

The reactions were performed in a standard quartz cuvette. 4-NP and $NaBH_4$ were added to 3 ml water to final concentrations of 100 µM and 20 mM respectively. The concentration of 4-NP was recorded at regular time intervals, by measuring absorbance at 400 nm on a UV5 UV-vis spectrometer, followed by conversion of absorbance to concentration using a predetermined standard calibration curve. Prior to use, washed bio-Pd samples were prepared as a stock suspension in deionised water, samples of which were digested with aqua regia, followed by quantification of palladium concentration by ICP-MS. Based on the measured stock concentration the volume of bio-Pd

suspension catalyst was added to the reaction to give a final concentration of 4 μM palladium.

3. Results

3.1 Bio-Pd Synthesis: Palladium Removal from Buffer Solutions by Cells

G. sulfurreducens removed TCP from all buffer solutions over time; the greatest decrease in palladium concentration was observed in TCP-TBS (>99%), then TCP-Bicarb (95%) and TCP-PBS (91%) (**Figure 1(a)**). The initial decrease in palladium concentration immediately after adding cells (biosorption at T = 0), was greatest in PBS (33%), then bicarbonate (26%) and was lowest in TBS (8%). Most removal of palladium from solution occurred within 3 h, with all bottles turning dark brown or black in colour (Figure S1A in the Supplementary Information), indicative of bioreduction of Pd(II) to Pd(0). In the absence of cells, the buffer solutions demonstrated differing effects on the solubility of palladium. In bicarbonate buffer Pd(II) gradually precipitated, with >99% palladium lost from solution by 24 h. The orange-brown precipitate observed (Figure S1A in the Supplementary Information) was likely a mixture of various Pd(II) chloro-aqua (Pd-Cl-H_2O) and hydroxy-chloride (Pd-Cl-OH) polynuclear complexes (12, 22–26). TCP-PBS solution was orange; no visible precipitate formed although the measured concentration of soluble palladium fell by around 29%. TCP-TBS solution was colourless throughout with >90% palladium remaining in solution, indicating that TBS complexed Pd(II) effectively and inhibited adsorption to the cells. After adding the acidic TCP stock solution (pH 3.58) to the reaction bottles the pH fell immediately in all three buffers, from a starting pH of 7.2 (**Figure 1(b)**). At 1 h in TCP-PBS and TCP-TBS the pH had dropped further, potentially due to biosorption of Pd(II) to the cells, as ligand exchange reactions between Pd(II) complexes and carboxylic acid, hydroxyl and protonated amine groups at the cell surface could release H^+ ions (27, 28). After 1 h, the pH began to increase in all reactions, in particular in TCP-Bicarb.

G. sulfurreducens removed less TAP from solution than TCP in the presence of bicarbonate and TBS

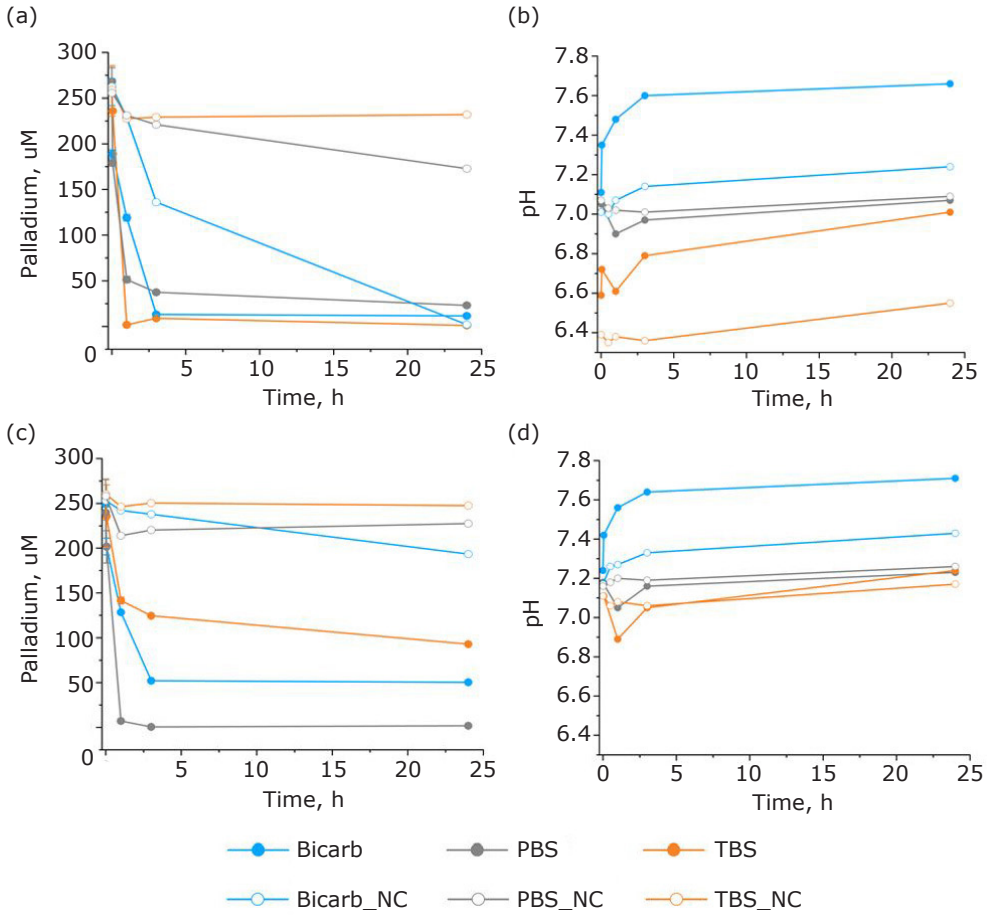

Fig. 1. (a) Change in palladium concentration in solution supplied with 250 μM of Na_2PdCl_4 in bicarbonate, PBS and TBS buffers, with and without (NC) *G. sulfurreducens*; (b) pH measurements of Na_2PdCl_4 in bicarbonate, PBS and TBS buffers, with and without cells; (c) change in palladium concentration in solution supplied with 250 μM of $Pd(NH_3)_4Cl_2{\cdot}H_2O$ in bicarbonate, PBS and TBS buffers, with and without (NC) *G. sulfurreducens*; (d) pH measurements of $Pd(NH_3)_4Cl_2{\cdot}H_2O$ in bicarbonate, PBS and TBS buffers, with and without cells

buffers, with 80% TAP-Bicarb and 63% TAP-TBS removed, respectively. However, palladium removal increased in the presence of PBS buffer, with >99% TAP-PBS removed from solution (**Figure 1(c)**). The initial decrease in palladium concentration immediately after adding cells (biosorption at T = 0) was lower in all samples for TAP than for TCP, with 19% removal in bicarbonate, 16% in PBS and was lowest in TBS (7%). Most palladium removal occurred within 3 h, with all bottles turning dark brown to black in colour (Figure S1B in the Supplementary Information). In the absence of cells, less TAP was lost from solution than TCP, with bicarbonate (21%) resulting in greater loss of palladium from solution than PBS (11%) and TBS (5%). Reaction bottles remained colourless throughout, and no precipitation was observed in the no cell controls with TAP (Figure S2B in the Supplementary Information). The pH was higher with TAP than TCP throughout all reactions (**Figure 1(d)**), as the TAP stock was less acidic (pH 5.68) and some ammonia ligands may also have been lost into solution upon addition to reaction bottles (29). The same general trends were observed for changes in pH with TAP containing reactions compared to TCP reactions, although the pH was consistently higher with TAP.

3.2 Ultraviolet-Visible Spectroscopy: Pd(II) Speciation in Buffer Solutions

To better understand how the selected biological buffers change the speciation of Pd(II) in solution, UV-vis spectroscopy was performed. The TCP stock solution did not contain the characteristic ligand-to-metal charge transfer (LMCT) bands for $[PdCl_4]^{2-}$ at 222 nm and 280 nm (9, 30). Rather, the strong absorbance band at 205–212 nm and shoulder at 230–240 nm (Figure S2D in the Supplementary Information), correspond to LMCT bands of Pd(II) chloro-aqua species such as $[PdCl_3(H_2O)]^-$ and $[PdCl_2(H_2O)_2]^0$ (9, 23, 24, 31). The weak metal-centred absorbance bands at 310 nm and 420 nm are typical of $[PdCl_3(H_2O)]^-$ in water and are seen as a result of rapid aquation (<1 s) of $[PdCl_4]^2$ to $[PdCl_3(H_2O)]^-$, which itself is subsequently hydrolysed to $[PdCl_3(OH)]^{2-}$, at circumneutral pH (12, 32).

TCP-Bicarb gave a strong LMCT peak at 249 nm at T = 0, which lost intensity over time until it became a broad shoulder at 256 nm (Figure S2A in the Supplementary Information), suggesting that hydrolysis to hydroxy-chloro species had occurred, such as $[PdCl_3(OH)]^{2-}$ and $[PdCl_2(OH)_2]^{2-}$ (23, 33). In addition, the increase in background absorbance observed is likely due to the formation of polynuclear hydroxide complexes (12, 26). The spectra of TCP-PBS contained two strong LMCT peaks at 230 nm and 280 nm, which are indicative of $[PdCl_3(OH)]^{2-}$ (22, 33). The loss of absorbance in these bands over time suggests further hydrolysis of this complex, or complexation by phosphate ions.

The TAP stock solution spectra contained a metal-centred absorbance band at 295 nm that corresponds to $[Pd(NH_3)_4]^{2+}$ (Figure S3D in the Supplementary Information) (29, 34). The $[Pd(NH_3)_4]^{2+}$ complex is stable in water, although after 3 h a slight drop in intensity may indicate slow change. TAP is much less stable in bicarbonate buffer as the metal-centred band at 300 nm at T = 0 shifted after 30 min, becoming a broad absorbance band stretching from 300–360 nm that corresponds to the Pd(II) ammonia-aqua complexes $[Pd(NH_3)_3(H_2O)]^{2+}$ and $[Pd(NH_3)_2(H_2O)_2]^{2+}$ at 317 nm and 341 nm, respectively (Figure S3A in the Supplementary Information) (29). The spectra of TAP-PBS and TAP-TBS were almost identical and did not contain any visible peaks in the range measured.

3.3 Bio-Pd Size and Agglomeration

TEM and XRD revealed that all bio-Pd samples contained small primary nanoparticles with mean sizes <6 nm (**Table I**). Bio-Pd from TCP-Bicarb possessed the smallest mean particle size and highest monodispersity, 3.7 ± 1.0 nm, and was comprised of many single nanoparticles and small agglomerates (**Figure 2(a)**). In comparison, TAP-Bicarb bio-Pd possessed a larger particle size distribution and mean size (5.7 ± 2.0 nm); also particles agglomerated more, compared to TCP-Bicarb, into both large (50–100 nm) and smaller (~10–20 nm) agglomerates (**Figure 2(b)**). Few single nanoparticles were observed in TCP-PBS with most agglomerated into small clusters of

Table I Mean Particle Size and Standard Distribution of Bio-Pd from Transmission Electron Microscopy and X-ray Diffraction

Sample	TEM, nm	XRD, nm
TCP-Bicarb	3.7 ± 1.0	3.9 ± 0.3
TCP-PBS	4.0 ± 1.0	5.8 ± 0.9
TCP-TBS	4.4 ± 0.9	5.4 ± 0.6
TAP-Bicarb	5.7 ± 2.0	6.1 ± 0.6
TAP-PBS	5.2 ± 1.2	6.4 ± 1.1
TAP-TBS	4.2 ± 1.3	4.0 ± 0.6

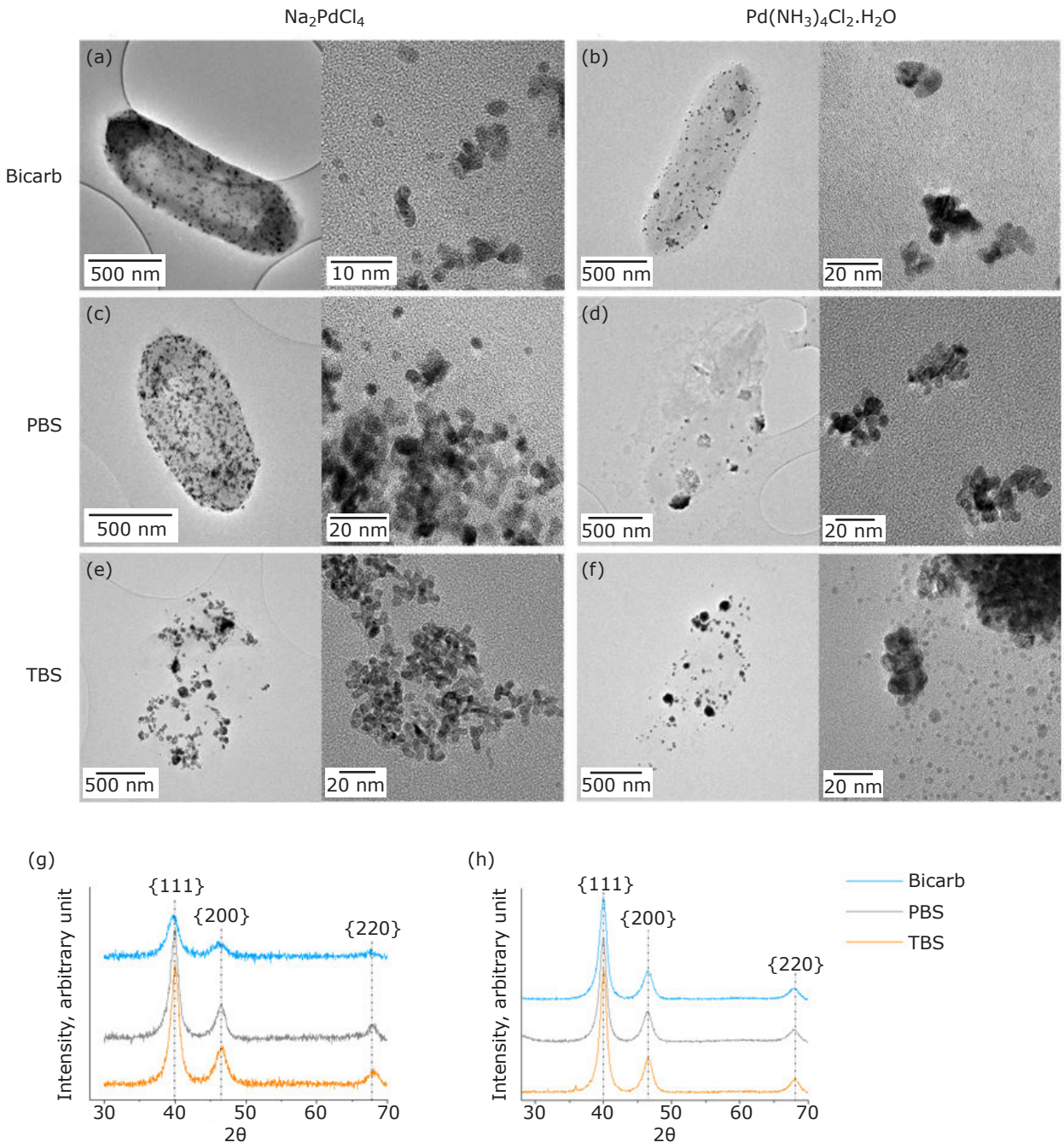

Fig. 2. (a) TEM of bio-Pd nanoparticles synthesised from TCP solution at high and low magnification in bicarbonate buffer; (b) TEM of bio-Pd nanoparticles synthesised from TAP solution at high and low magnification in bicarbonate buffer; (c) TEM of bio-Pd nanoparticles synthesised from TCP solution at high and low magnification in PBS buffer; (d) TEM of bio-Pd nanoparticles synthesised from TAP solution at high and low magnification in PBS buffer; (e) TEM of bio-Pd nanoparticles synthesised from TCP solution at high and low magnification in TBS buffer; (f) TEM of bio-Pd nanoparticles synthesised from TAP solution at high and low magnification in TBS buffer; (g) XRD patterns of bio-Pd patterns from TCP in three buffers; (h) XRD patterns of bio-Pd patterns from TAP in three buffers

nanoparticles (**Figure 2(c)**), whereas in TAP-PBS, particles formed much larger agglomerates, with some measuring >100 nm (**Figure 2(d)**). TCP-TBS bio-Pd was mostly agglomerated into >50 nm clusters, and few single particles were observed (**Figure 2(e)**). However, in TAP-TBS many single particles were seen amongst large >50 nm agglomerates (**Figure 2(f)**).

The typical intact rod-shaped cell structure of *G. sulfurreducens* was seen under TEM in all samples

except for TAP-PBS and TCP-TBS where the cell structure appeared to be extremely compromised. Cell lysis appears to have occurred during the reaction with Pd(II) in TCP-TBS (**Figure 2(e)**). Less cell lysis appeared to have occurred in TAP-PBS, however, crystals appeared to have precipitated on and extended out from the cells (**Figure 2(d)**). In contrast, TAP-TBS and TCP-PBS cells appeared to have retained the integrity of their cell structure, indicating that specific palladium complexes may be damaging to cells. A limitation of this study was the use of drop cast whole cell samples only, as they do not show the location of particles in relation to the inner and outer membranes of the Gram-negative *G. sulfurreducens*. Acetate-driven bioreduction would be expected to produce bio-Pd at the outer membrane, as the extracellular electron transfer chain of *G. sulfurreducens* that utilises acetate as an electron donor terminates at the periphery of the cell, however, TEM on ultrathin sectioned samples would be necessary to prove this.

3.4 Bio-Pd Oxidation State

XPS analysis revealed the oxidation states of palladium in bio-Pd samples to be a mixture of Pd(0) and Pd(II) (**Table II**). The bio-Pd samples predominantly consisted of Pd(0) at a binding energy range of 334.7–334.9 eV. The peak for Pd(II), at a binding energy range of 337.5–337.9 eV, could not be assigned to a specific Pd(II) species. Bio-Pd synthesised from TCP and TAP in PBS possessed very similar palladium 3d XPS spectra, with almost identical ratios of Pd(0):Pd(II). TBS on the other hand produced quite different spectra; TCP-TBS had the highest amount of Pd(0), 92%, compared to TAP-TBS which contained 73% Pd(0). Bicarbonate bio-Pd contained the highest proportion of unreduced Pd(II), with TCP-Bicarb possessing 61% Pd(0) and TAP-Bicarb containing 69% Pd(0).

3.5 Bio-Pd Catalysis: 4-Nitrophenol Reduction

To assess the catalytic activity of the various bio-Pd nanoparticles synthesised under different solution chemistries by *G. sulfurreducens*, the reduction of 4-NP to 4-aminophenol (4-AP) was performed, with $NaBH_4$ as the hydrogen donor. Bio-Pd synthesised in bicarbonate buffer gave the most complete 4-NP reduction, with both TCP-Bicarb and TAP-Bicarb demonstrating near complete reactions after 60 min (**Figure 4**). However, TCP-Bicarb gave a much faster initial rate of reaction than TAP-Bicarb, 0.34 min^{-1} and 0.14 min^{-1}, respectively. The next most active catalyst was TCP-PBS, which slightly outperformed TAP-TBS in terms of both extent of reduction and initial rate (**Table III**). However, a sharp drop off in catalytic activity was then observed for TCP-TBS, followed by TAP-PBS, with 45% and 38% 4-NP reduced, respectively.

4. Discussion

Metal nanoparticle biosynthesis studies often fail to consider that some metal complexes are not stable in aqueous solution and undergo stepwise hydration and hydrolysis reactions (35). As shown in the UV-vis spectra, TCP rapidly transforms to $[PdCl_3(H_2O)]^-$ in water, which is stable for a few hours but will hydrolyse further and form

Table II X-ray Photoelectron Spectroscopy Analysis Showing the Percentage Composition of Pd(0)/Pd(II) in Bio-Pd and the Corresponding Peak Binding Energy for Bio-Pd

Sample	Oxidation state	Composition, %	3d 5/2 binding energy, eV
TCP-Bicarb	Pd(0)	61	334.8
	Pd(II)	39	337.5
TCP-PBS	Pd(0)	82	334.9
	Pd(II)	18	337.8
TCP-TBS	Pd(0)	92	334.9
	Pd(II)	8	337.9
TAP-Bicarb	Pd(0)	69	334.7
	Pd(II)	31	337.7
TAP-PBS	Pd(0)	83	334.9
	Pd(II)	17	337.8
TAP-TBS	Pd(0)	73	334.8
	Pd(II)	27	337.6

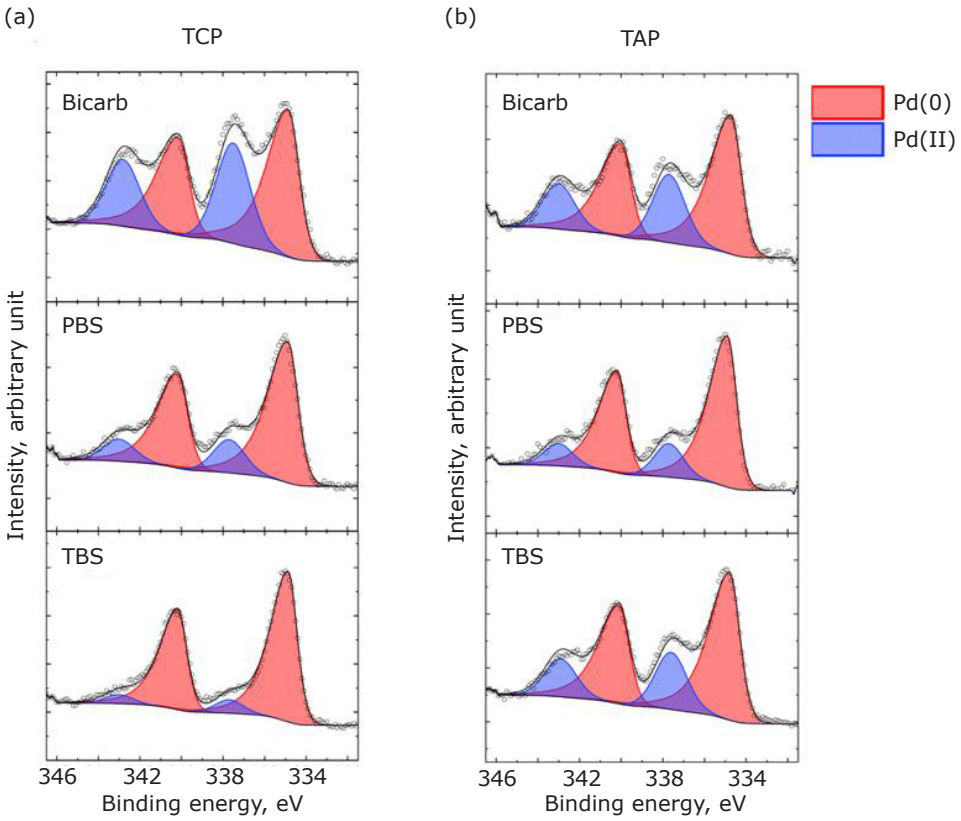

Fig. 3. XPS analysis of the palladium 3d spectra of bio-Pd from: (a) TCP; and (b) TAP synthesised in bicarbonate buffer, PBS and TBS

polynuclear hydroxyl species; it is therefore necessary to make up TCP solutions just before use (12). In comparison, TAP was shown to be much more stable in water. Crucially, this study shows that the speciation of these Pd(II) salts changes drastically upon the addition of common buffers used in biological studies, either due to enhancing hydrolysis and hydration reactions i.e. bicarbonate buffer, or direct complexation by the buffer such as by TBS. Therefore assumptions made about the solution chemistry and speciation of Pd(II) based upon the starting materials (palladium salt and buffer solution), the subsequent interactions of these palladium species with cells and the catalytic properties of the resulting nanoparticles synthesised, requires more careful consideration.

Complexation of Pd(II) in buffer solutions can alter the physical and chemical properties of Pd(II), which can impact the subsequent microbe-metal interactions. The charge on the Pd(II) complex may change, affecting the electrostatic binding site of the complex at the cell surface. The ligands of the Pd(II) complex can also affect coordination to functional groups at the cell surface, and subsequent ligand exchange reactions. The ligand sets of Pd(II) complexes will also affect the reduction potential of Pd(II), which may in turn impact the ability of microbial electron transfer proteins to reduce the metal. Starting from $[PdCl_4]^{2-}$ with a reduction potential of 0.62 V *vs*. standard hydrogen electrode (SHE), hydration of TCP to chloro-aqua species raises the reduction potential to 0.91 V *vs*. SHE for fully hydrated $[Pd(H_2O)_4]^{2+}$, whereas hydrolysis of TCP lowers the reduction potential to 0.1 V *vs*. SHE for fully hydrolysed $[Pd(OH)_4]^{2-}$ (35, 36). On the other hand, the reduction potential of $[Pd(NH_3)_4]^{2+}$ is 0 V *vs*. SHE, which similar to TCP increases upon hydration (36). The variation in reduction potential of the different Pd(II) complexes may be a factor in the variation of Pd(0):Pd(II) ratios observed in the bio-Pd samples (**Figure 3**).

The most profound effect of varying the solution chemistry in the synthesis of bio-Pd was on the catalytic properties. The extent of nanoparticle agglomeration was the most important factor as all samples possessed mean particle sizes of <6 nm. Bicarbonate buffer enhanced the hydrolysis and hydration of Pd(II) but did not appear to directly complex Pd(II). Bio-Pd from TCP-Bicarb possessed the smallest mean particle size and lowest amount of agglomeration and gave the highest conversion and initial rate of reaction. The bioreduction of TAP resulted in large agglomerates forming, hence TAP-Bicarb possessed a slower initial reaction rate than TCP-Bicarb. TCP-PBS reduced less 4-NP (90%) than TCP-Bicarb with

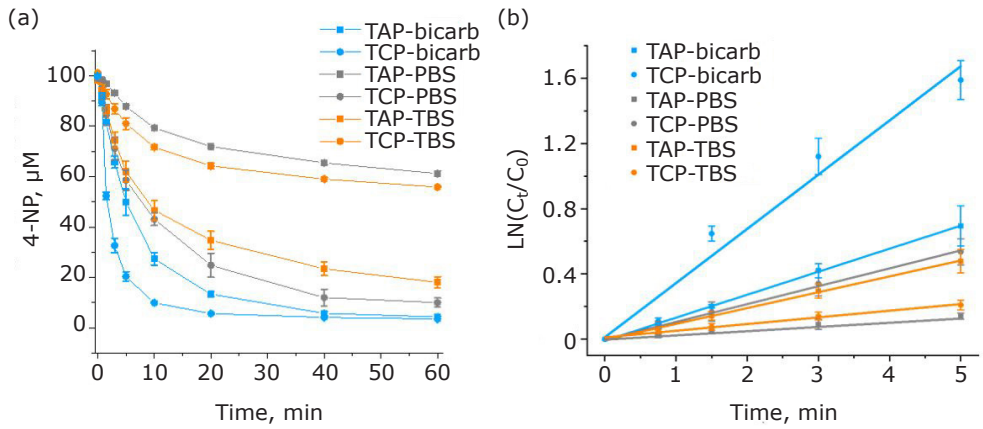

Fig. 4. Catalytic performance of bio-Pd nanoparticles for the reduction of 4-NP to 4AP; all reactions were normalised to 4 μM palladium: (a) reaction profile; (b) initial rate of reaction

Table III The Percentage Amount of 4-Nitrophenol Reduced by Bio-Pd after 60 min and the Initial Rate of Reaction after 5 min

Sample	TCP-Bicarb	TAP-Bicarb	TCP-PBS	TAP-PBS	TCP-TBS	TAP-TBS
4-NP reduced, %	97	96	90	38	45	82
Initial rate, min^{-1}	0.34	0.14	0.11	0.03	0.04	0.10

a third of the initial reaction rate (**Figure 4**), despite measuring a similar size distribution (Figure S4 in the Supplementary Information), due to possessing few single nanoparticles and mostly small agglomerates. Similarly, bio-Pd from TAP-PBS and TCP-TBS possessed mostly large agglomerates of particles and gave the slowest and least extent of reaction for 4-NP reduction. Another consideration to explain relatively poor catalytic performance is the cell integrity following reaction with Pd(II), with significant cell lysis observed in TEM of the TAP-PBS and TCP-TBS systems. Previously, authors have proposed that the release of biomolecules from cells could poison the catalyst surface (37, 38).

5. Conclusions

In this study we demonstrate that palladium solution chemistry plays an important and previously overlooked role in the bioreduction of Pd(II) and the properties of the resulting nanoparticles. As such, the choice of chemical reagents and solutions should be carefully considered to fine-tune the properties of biotechnologically synthesised palladium nanoparticles. Here it was shown that different combinations of Pd(II) salts and biological buffers resulted in bio-Pd from *G. sulfurreducens* with different mean sizes, extent of agglomeration and ratios of Pd(0):Pd(II), and crucially, this controlled the catalytic activity of the nanoparticles for 4-NP reduction. Essential to explaining these results is the understanding that not only does Pd(II) undergo hydration and hydrolysis reactions in solution, but that Pd(II) specifically reacts with components present in many commonly used biological buffers. The speciation of Pd(II) was therefore different in each sample, resulting in contrasting bioreduction endpoints. In summary, the Pd(II) starting material and buffer interact, changing the metal speciation and subsequent metal-microbe interaction, resulting in different nanoparticle morphologies, which changes the catalytic activity of the resulting bio-Pd nanoparticles.

Conflicts of Interest

There are no conflicts to declare.

Acknowledgements

The authors would like to thank the Engineering & Physical Sciences Research Council (EPSRC) and Johnson Matthey, UK, for funding of the PhD iCASE studentship award for Christopher Egan-Morriss, and the Biotechnology and Biological Sciences Research Council (BBSRC) for funding from the grants BB/L013711/1 and BB/R010412/1. Electron microscopy access was supported by the Henry Royce Institute for Advanced Materials, funded through EPSRC grants EP/R00661X/1, EP/S019367/1, EP/P025021/1 and EP/P025498/1.

References

1. J. R. Lloyd, J. M. Byrne, V. S. Coker, *Curr. Opin. Biotechnol.*, 2011, **22**, (4), 509
2. C. Egan-Morriss, R. L. Kimber, N. A. Powell, J. R. Lloyd, *Nanoscale Adv.*, 2022, **4**, (3), 654
3. J. R. Lloyd, P. Yong, L. E. Macaskie, *Appl. Environ. Microbiol.*, 1998, **64**, (11), 4607
4. W. De Windt, P. Aelterman, W. Verstraete, *Environ. Microbiol.*, 2005, **7**, (3), 314
5. A. M. Pat-Espadas, E. Razo-Flores, J. R. Rangel-Mendez, F. J. Cervantes, *Appl. Microbiol. Biotechnol.*, 2012, **97**, (21), 9553
6. Y. Tuo, G. Liu, J. Zhou, A. Wang, J. Wang, R. Jin, H. Lv, *Bioresour. Technol.*, 2013, **133**, 606
7. K. Deplanche, J. A. Bennett, I. P. Mikheenko, J. Omajali, A. S. Wells, R. E. Meadows, J. Wood, L. E. Macaskie, *Appl. Catal. B: Environ.*, 2014, **147**, 651
8. C. Colombo, C. J. Oates, A. J. Monhemius, J. A. Plant, *Geochem.: Explor. Environ. Anal.*, 2008, **8**, (1), 91
9. L. I. Elding, L. F. Olsson, *J. Phys. Chem.*, 1978, **82**, (1), 69
10. R. M. Izatt, D. Eatough, J. J. Christensen, *J. Chem. Soc. A*, 1967, 1301
11. D. W. Barnum, *Inorg. Chem.*, 1983, **22**, (16), 2297
12. F. Kettemann, M. Wuithschick, G. Caputo, R. Kraehnert, N. Pinna, K. Rademann, J. Polte, *CrystEngComm*, 2015, **17**, (8), 1865
13. C. M. H. Ferreira, I. S. S. Pinto, E. V. Soares, H. M. V. M. Soares, *RSC Adv.*, 2015, **5**, (39), 30989
14. R. E. Wildung, Y. A. Gorby, K. M. Krupka, N. J. Hess, S. W. Li, A. E. Plymale, J. P. McKinley, J. K. Fredrickson, *Appl. Environ. Microbiol.*, 2000, **66**, (6), 2451
15. L. Shi, S. M. Belchik, A. E. Plymale, S. Heald, A. C. Dohnalkova, K. Sybirna, H. Bottin, T. C. Squier, J. M. Zachara, J. K. Fredrickson, *Appl. Environ. Microbiol.*, 2011, **77**, (16), 5584
16. C. Engelbrekt, K. H. Sørensen, J. Zhang, A. C. Welinder, P. S. Jensen, J. Ulstrup, *J. Mater. Chem.*, 2009, **19**, (42), 7839
17. C. Engelbrekt, K. H. Sørensen, T. Lübcke, J. Zhang, Q. Li, C. Pan, N. J. Bjerrum, J. Ulstrup, *ChemPhysChem*, 2010, **11**, (13), 2844
18. J. I. B. Janairo, K. Sakaguchi, *Chem. Lett.*, 2014, **43**, (8), 1315
19. A. G. Delgado, P. Parameswaran, D. Fajardo-Williams, R. U. Halden, R. Krajmalnik-Brown, *Microb. Cell Fact.*, 2012, **11**, 128
20. C.-H. Liao, L. M. Shollenberger, *Lett. Appl. Microbiol.*, 2003, **37**, (1), 45
21. B. E. Fischer, U. K. Häring, R. Tribolet, H. Sigel, *Eur. J. Biochem.*, 1979, **94**, (2), 523
22. J.-F. Boily, T. M. Seward, J. M. Charnock, *Geochim. Cosmochim. Acta*, 2007, **71**, (20), 4834
23. C. J. le Roux, R. J. Kriek, *Hydrometallurgy*, 2017, **169**, 447
24. C. Drew Tait, D. R. Janecky, P. S. Z. Rogers, *Geochim. Cosmochim. Acta*, 1991, **55**, (5), 1253
25. J. M. van Middlesworth, S. A. Wood, *Geochim. Cosmochim. Acta*, 1999, **63**, (11–12), 1751
26. P. A. Simonov, S. Y. Troitskii, V. A. Likholobov, *Kinet. Catal.*, 2000, **41**, (2), 255
27. J. Wang, S. Bi, Y. Chen, Y. Hu, *Ecotoxicol. Environ. Saf.*, 2020, **190**, 110124
28. A. Sari, D. Mendil, M. Tuzen, M. Soylak, *J. Hazard. Mater.*, 2009, **162**, (2–3), 874
29. L. Rasmussen, K. Jørgensen, *Acta Chem. Scand.*, 1968, **22**, (7), 2313
30. J.-F. Boily, T. M. Seward, *Geochim. Cosmochim. Acta*, 2005, **69**, (15), 3773
31. J. J. Cruywagen, R. J. Kriek, *J. Coord. Chem.*, 2007, **60**, (4), 439
32. R. H. Byrne, W. Yao, *Geochim. Cosmochim. Acta*, 2000, **64**, (24), 4153
33. C. J. le Roux, R. J. Kriek, *Hydrometallurgy*, 2019, **186**, 21
34. D. Spielbauer, H. Zeilinger, H. Knoezinger, *Langmuir*, 1993, **9**, (2), 460
35. J. Richard-Daniel, D. Boudreau, *ChemNanoMat*, 2020, **6**, (6), 907
36. V. Yadav, S. Jeong, X. Ye, C. W. Li, *Chem. Mater.*, 2022, **34**, (4), 1897
37. S. De Corte, S. Bechstein, A. R. Lokanathan, J. Kjems, N. Boon, R. L. Meyer, *Colloids Surf. B: Biointerfaces*, 2013, **102**, 898
38. L. S. Søbjerg, A. T. Lindhardt, T. Skrydstrup, K. Finster, R. L. Meyer, *Colloids Surf. B: Biointerfaces*, 2011, **85**, (2), 373

The Authors

Chris Egan-Morriss received his MEng degree in Materials Science and Engineering with Biomaterials from the University of Manchester, UK, in 2019. He is currently a PhD candidate under Professor Jon Lloyd in the Department of Earth and Environmental Sciences at the University of Manchester, and is the recipient of an iCASE award with Johnson Matthey, UK. His research interests are biological metal recovery and synthesis of metal nanoparticles and their applications in sustainable biotechnologies.

Richard L. Kimber completed his PhD in Geomicrobiology at the University of Manchester in 2012, under the supervision of Professor Jon Lloyd. Following this, he worked as a postdoctoral researcher at the University of Vienna, Austria, before returning to the University of Manchester to work as a postdoc on microbial synthesis of nanoparticle catalysts, with a particular focus on copper and palladium. Since 2020, Richard is a Junior Group Leader in the Department of Environmental Geosciences at the University of Vienna. His current interests include microbial interactions with metals and DNA interactions at mineral surfaces.

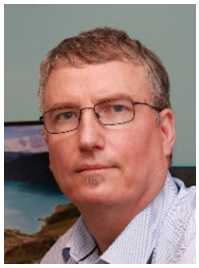

Nigel A. Powell received his PhD in Chemistry from the University of Southampton, UK, following studies on the coordination chemistry of iridium and platinum. After carrying out postdoctoral research at the University of Manchester, he moved to industry and is currently eleven years into his second spell at Johnson Matthey. He has a long-term interest in the interaction of metals with biological systems and in particular the bringing together of biology and chemistry to improve the sustainability of industrial processes.

Jonathan R. Lloyd is Professor of Geomicrobiology at the University of Manchester. He trained as a microbiologist at the University of Bath, UK, (BSc) and the University of Kent, UK, (PhD), before postdoctoral work at the University of Birmingham, UK, and the University of Massachusetts Amherst, USA. He has worked in Manchester for 20 years, and leads a multidisciplinary group working across the physical and life sciences. He has a particular interest in the biotechnological potential of metal-reducing microbes isolated from the Earth's subsurface, recognised by awards including the Schlumberger (Mineralogical Society) and Bigsby (Geological Society) medals. Current work includes using these microbes to recover waste metals as valuable nanoparticles.